UvA-DARE (Digital Academic Repository)

Aluminum Incorporation in the Si-Nl10 Thermal Donor

Gregorkiewicz, T.; Bekman, H.H.P.T.; Ammerlaan, C.A.J.

Link to publication

Aluminum incorporation in the Si-NL10 thermal donor

T. Gregorkiewicz, H. H. P. Th. Bekman, and C. A. J. Ammerlaan
Van der Waals–Zeeman Laboratorium der Universiteit van Amsterdam,
Valckenierstraat 65-67, NL-1018 XE Amsterdam, The Netherlands

The role of aluminum dopants in the creation and properties of the Si-NL10 center was investigated by means of electron-nuclear-double-resonance techniques. At least 10 different Si-NL10 species were identified, and their generation kinetics were studied in detail. Possible transformation mechanisms were considered. The existence of the Si-NL10 centers not containing aluminum was inferred from indirect evidence. The generation of the Si-NL10 centers in heavily aluminum-doped silicon was also investigated, providing further evidence against a unique correlation of these centers with aluminum-oxygen complexes.

I. INTRODUCTION

When oxygen-rich silicon is subjected to thermal annealing, various defects can be created, depending on the heat-treatment temperature (and thermal history of the sample). At moderately low temperature between 300 °C and 500 °C the so-called thermal donors are generated.[1] Infrared measurements[2] showed that there are many (up to 12) different thermal-donor species of double-donor, effective-mass character. The early electron-paramagnetic-resonance (EPR) study of Muller et al.[3] identified a few paramagnetic resonance spectra, two of which, Si-NL8 and Si-NL10, were subsequently shown to be related to the thermal donors.[4] Later investigations by electron-nuclear double resonance (ENDOR) identified hyperfine interactions with oxygen nuclei for both spectra.[5,6] EPR measurements under uniaxial stress by Lee, Trombetta, and Watkins[7] connected Si-NL8 to the singly ionized state of the thermal double donor (TD^+), while the identity of the other paramagnetic center, Si-NL10, remained unclear. Further detailed ENDOR studies[8,9] led to microscopic models which suggested different structures of the two defects. However, a careful evaluation of the existing evidence showed that the available experimental data do not exclude a similar structure for the core of both defects.[10] The results are shown to allow the earlier suggested identification of the Si-NL10 EPR spectrum with another paramagnetic charge state of the thermal donor, possibly TD^-.[11] Such an identification coincided with the findings of Burger et al.[12] who postulated He^--type traps to be created by double-donor chalcogen complexes in silicon. However, a direct proof for the existence of TD^- is still missing and the identification of Si-NL10 remains speculative.

The most serious problem in the identification of the Si-NL10 center is the role played by aluminum, both in the generation and the structure of this center. The ENDOR study on Si-NL8 identified hyperfine interactions with ^{17}O and ^{29}Si nuclei; in addition to these, the ENDOR study of Si-NL10 performed in aluminum-doped silicon also revealed interactions with ^{27}Al nuclei. This finding raises serious doubts about whether Si-NL8 and Si-NL10 could originate from basically the same de-

fect. Furthermore, in their recent study, Claybourn and Newman[13] suggested that in heavily aluminum-doped Cz-Si ($[Al] > 10^{17}$ cm^{-3}), an aluminum-related kind of thermal donor was generated and that these (single) donors could be related to the Si-NL10 spectrum. In view of the apparent problem posed by the aluminum incorporation to the silicon thermal-donor issue in general and the mutual NL8↔NL10 relation in particular, the current study has been undertaken. The aim of this paper is the investigation of the peculiar behavior and role of aluminum in the heat-treatment center Si-NL10, with help of the EPR, ENDOR, and field-stepped ENDOR techniques.

Field-stepped ENDOR (FSENDOR) is one of the possible extensions of the (conventional) ENDOR technique. It can serve to obtain an image of the specific EPR line, or line component, which is related to a certain ENDOR transition. It can be used to separate partially overlapping resonance signals, originating from different centers, or from different EPR transitions or orientations superimposed in one experimentally observed resonance line.[14] In the former capacity it has been applied in the current study.

Although EPR intensities have qualitative rather than quantitative character, they can, under favorable conditions, also provide information about the concentration of the paramagnetic centers. The absolute concentration values as determined in this way should be treated as estimations only, with the accuracy not much better than the order of magnitude. A much higher accuracy may be achieved for the measurement of the relative changes of the concentration, in which case the same EPR signal is compared following, e.g, two somewhat different heat treatments. In such a situation, when extreme care is executed for reproducible operation of the spectrometer, variations as small as 10% may be meaningful.

In ENDOR the situation is more complex and the actual concentration of paramagnetic centers, although certainly related to the strength of the ENDOR signal, cannot be inferred from it. Nevertheless, the ENDOR experiment is reproducible, i.e., both the positions as well as *the intensities* of the observed resonances remain constant when measured under identical conditions. Moreover,

under given conditions, the ENDOR response represents a certain percentage of the EPR signal, which, as mentioned above, is *directly* related to the concentration. Therefore, the intensity of ENDOR signals could also reflect the concentration of the paramagnetic centers. The requirements include that for the centers to be compared the ENDOR must be observed under identical conditions. Furthermore, the spin-relaxation times governing the EPR and ENDOR processes must be equal, requiring centers of very similar structure. Also, care has to be taken that the ENDOR signals from equivalent shells are compared. When the above requirements are satisfied, it seems reasonable to expect that the intensity ratio of the ENDOR signals will be proportional to the number of interacting nuclei, i.e., the concentration of centers and the actual number of nuclei in a given shell. (Direct experimental confirmation of it can be found in the ^{29}Si ENDOR study of the negatively charged vacancy in silicon.[15]) Consequently, the intensity changes of these signals will be proportional to the variations of the concentration of the relevant centers. For the different thermal-donor species this particular favorable situation is expected to be realized. The present study is based on this assumption.

II. EXPERIMENT

A. Equipment

The measurements were performed with a superheterodyne spectrometer operating at 23 GHz and adjusted to detect the dispersion part of the EPR signal. The magnetic field, modulated at a frequency of 83 Hz, could be rotated in the $(0\bar{1}1)$ plane of the sample. A cylindrical TE_{011}-mode silver-coated epibond cavity was used. In the thin silver layer on the cylindrical sidewall of the cavity, a spiral groove was cut, making the sidewall suitable to serve as an ENDOR coil. For ENDOR measurements the radio frequency was square-wave modulated at 3.3 Hz to allow double phase-sensitive detection of the signal. The sample was held at 4.2 K. The ENDOR measurements could be performed under white-light illumination. Light from a halogen source was then transmitted to the sample by a quartz rod.

B. Samples

The samples used in the study were cut from commercial (Wacker Chemitronic) aluminum-doped Czochralski-grown silicon. The sample used for the ENDOR measurements was of $\rho \approx 3$–5 Ω cm resistivity with aluminum concentration $[Al] = 5 \times 10^{15}$ cm^{-3} and carbon concentration $[C] \leq 5 \times 10^{15}$ cm^{-3}. The interstitial oxygen concentration was $[O_i] \approx 1.2 \times 10^{18}$ cm^{-3}. For the EPR measurements a heavily aluminum-doped material (the heavily aluminum-doped Czochralski silicon used in this study was kindly provided by Dr. Werner Zulehner of Wacker Chemitronic) was used with resistivity of $\rho \approx 0.2$ Ω cm, aluminum concentration $[Al] \approx 2 \times 10^{17}$ cm^{-3}, carbon concentration $[C] \leq 5 \times 10^{15}$ cm^{-3}, and oxygen concentration $[O_i] \approx 8.5 \times 10^{17}$ cm^{-3}.

The samples had dimensions of $2 \times 2 \times 15$ mm^3 with the longest side corresponding to the $[0\bar{1}1]$ direction. Before the thermal-donor annealing, the samples were heated up to 1380 °C for half an hour. This was followed by a rapid quench to room temperature to disperse the interstitial oxygen. Finally, the samples were given heat treatments for various durations at 470 °C. In order to determine the concentration of the studied paramagnetic centers, a phosphorus-doped (10^{14} cm^{-3}) silicon sample was used as a calibration standard.

III. EXPERIMENTAL RESULTS

A. ENDOR

In the float-zone sample studied before, six different aluminum resonances could be observed.[8] Four of them were subjected to a detailed fitting. Figure 1 shows an ENDOR scan of the present Czochralski-grown sample after a thermal-donor generation anneal of 48 h at 470 °C. The scan was made for a single EPR orientation with the magnetic field along the [011] direction. Apart from the already known aluminum tensors, four more were identified. Due to a rather low signal-to-noise ratio, the new aluminum tensors were not traced over the entire $(0\bar{1}1)$ measuring plane; therefore, it is not possible to obtain their detailed hyperfine and quadrupole parameters. Figure 2 presents the level diagram for an $S = \frac{1}{2}$, $I = \frac{5}{2}$ system, which is appropriate for the aluminum ENDOR study of the Si-NL10 center. The ENDOR signals shown in Fig. 1 correspond to the NMR transition $9 \leftrightarrow 10$. Since (to first order) there is no quadrupole contribution to ENDOR transition $9 \leftrightarrow 10$, then it can be derived that

$$hf_{9 \leftrightarrow 10} = |g_N \mu_N B + \tfrac{1}{2} A_{\text{eff}}| . \tag{1}$$

The $\vec{A}$ tensors determined in the earlier study[8] were found to be very isotropic with a ratio of the isotropic to the anisotropic part $a/b \approx 20$. Therefore, if we neglect the anisotropic part, we can make a rough estimate of the
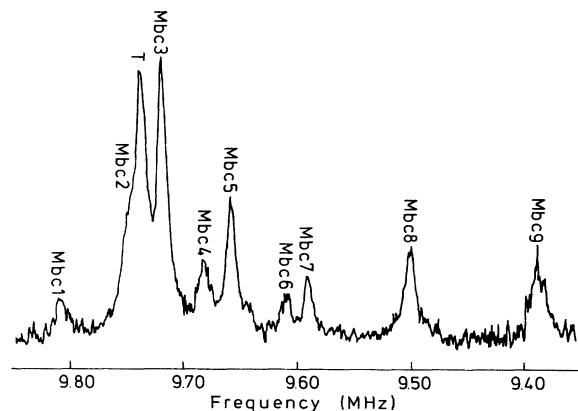

FIG. 1. ENDOR spectrum of the Cz-Si:Al sample after 48-h heat treatment at 470 °C. Ten different aluminum resonance lines can be distinguished, corresponding to ten different Si-NL10 thermal-donor species. The magnetic field **B** is along the [011] crystallographic direction, $B = 821.5$ mT.

$$E = m_S g_{eff} \mu_B B - m_I g_N \mu_N B + m_S m_I A_{eff} + m_I^2 Q_{eff}$$
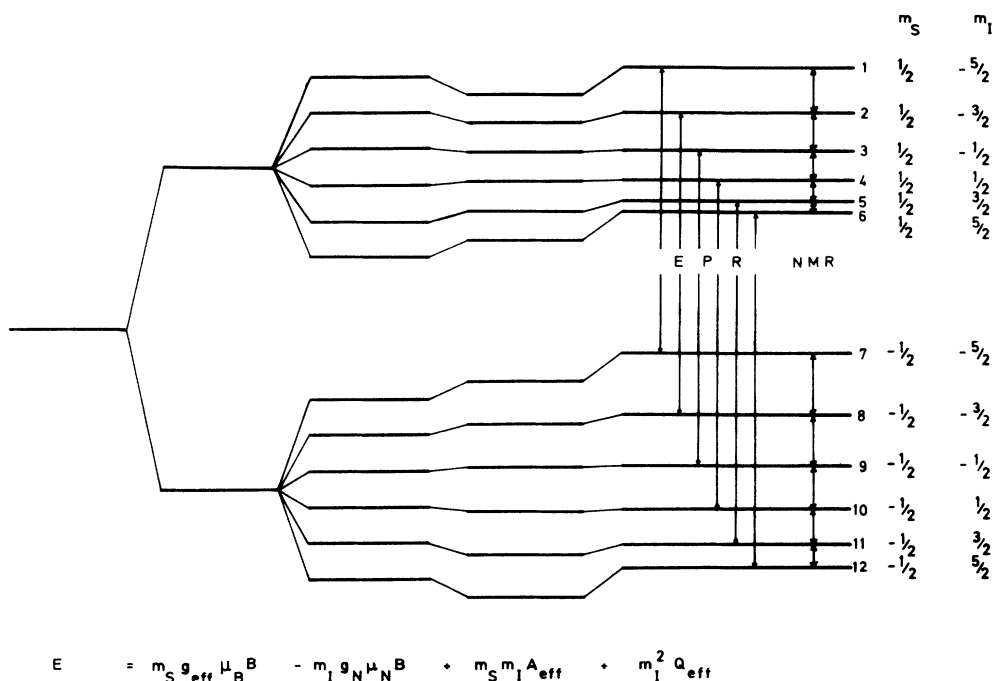
FIG. 2. Energy-level diagram for a system with electron spin $S = \frac{1}{2}$ and nuclear spin $I = \frac{5}{2}$.

isotropic a values of the other tensors which were found in the current experiment by using Eq. (1) and the experimentally determined ENDOR frequencies for transition $9 \leftrightarrow 10$. The results are collected in Table I. The values given in the last column in the table incorporate a correction factor in order to provide some compensation for the very rough determination procedure. The size of the correction has been determined by comparing the a values predicted for the T and $Mbc3$ tensors with those actually found by detailed fitting. The correction has been further applied to the $Mbc4$ to $Mbc9$ tensors because of their very close resemblance to the $Mbc3$ and T shells. (The $Mbc1$ and $Mbc2$ tensors have a slightly higher degree of anisotropy.) Due to the rather primitive

TABLE I. The isotropic part a of the hyperfine interaction for the aluminum shells as determined in the current study. The units are kHz. f_z denotes the Zeeman frequency for the aluminum nuclei ($=g_N \mu_N B/h$). The "fitted" a values are taken from Ref. 8. For the correction procedure see text.

Tensor	$f_{9 \to 10} - f_z$	A_{eff}/h	a/h Fitted	a/h Corrected
$Mbc1$	692	1384	1417	
$Mbc2$	633	1266	1307	
T	619	1238	972	982
$Mbc3$	601	1202	964	953
$Mbc4$	563	1126		893
$Mbc5$	539	1078		855
$Mbc6$	~492	984		781
$Mbc7$	472	944		749
$Mbc8$	382	764		606
$Mbc9$	265	530		421

procedure of their determination, the a values as collected in Table I should be treated as indicative numbers only.

The Si-NL10 EPR center has orthorhombic symmetry with six different defect orientations possible within the silicon lattice. A hyperfine interaction with a nearby magnetic nucleus, like ^{27}Al, ^{17}O, or ^{29}Si, can lower the symmetry. In general, four different cases are possible; for the present study only two of them are important. Figures 3(a) and 3(b) present the expected ENDOR patterns if a single, nondegenerate EPR orientation is followed for a hyperfine interaction which does not change the orthorhombic ($2mm$) symmetry or lowers it to monoclinic (m), respectively. In the previous experiment[8] it was shown that among the six identified aluminum hyperfine shells, only one (Al-T) was of the orthorhombic symmetry type, while all the others (Al-$Mbc1$ to 5) were of monoclinic symmetry. All the aluminum hyperfine shells identified in this study—Al-$Mbc6$ to 9—were found also to be of the monoclinic symmetry type. Figure 4 illustrates how this conclusion was reached for the Al-$Mbc7$ and -$Mbc8$ tensors. In the figure the magnetic field is either along the [011] direction or moved three degrees away from the [011] direction; as can be seen, the aluminum interactions are split into two ENDOR signals, which, as illustrated by Fig. 3, provides evidence for the monoclinic symmetry type.

B. Field-stepped ENDOR

ENDOR transition $9 \leftrightarrow 10$ attains its maximum intensity for the EPR transitions $3 \leftrightarrow 9$ and $4 \leftrightarrow 10$. In the first-order approximation these EPR transitions are given by
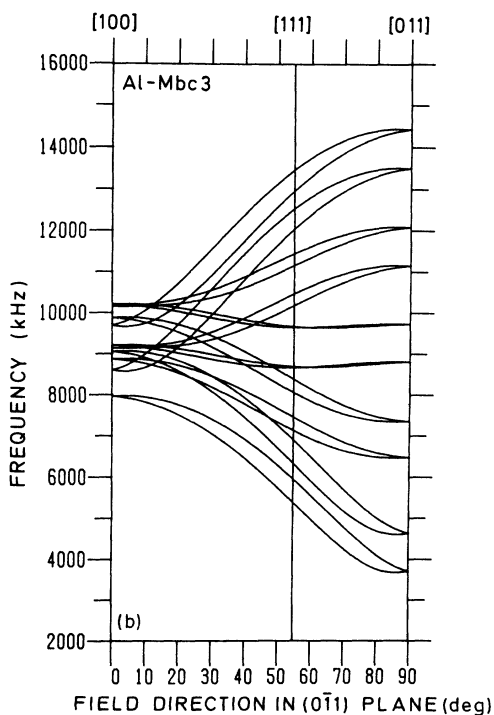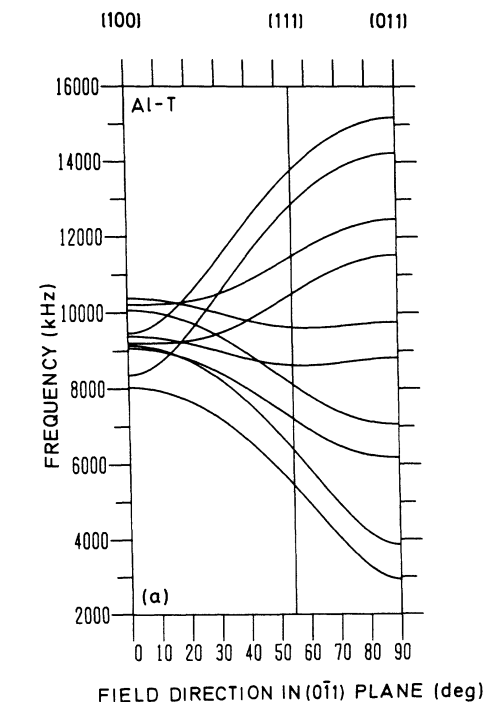
FIG. 3. Angular ENDOR pattern expected for a single non-degenerate EPR orientation in case of a hyperfine interaction of (a) orthorhombic (tensor T) and (b) monoclinic (tensor $Mbc3$) symmetry type.
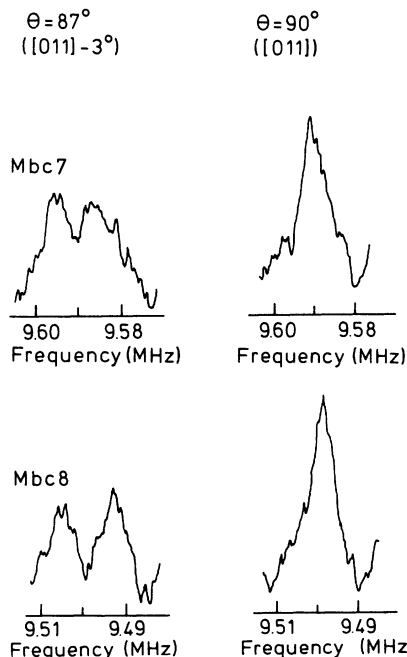

FIG. 4. Experimental evidence for a monoclinic symmetry type of the newly found tensors Al-$Mbc7$ and 8. A splitting of the resonance lines can be noted when the direction of the magnetic field is tilted away by 3° from the [011] crystallographic axis.

$$h\nu_{3\leftrightarrow9} = g_{eff}\mu_B B - \tfrac{1}{2}A_{eff} \qquad (2)$$

and

$$h\nu_{4\leftrightarrow10} = g_{eff}\mu_B B + \tfrac{1}{2}A_{eff} . \qquad (3)$$

Therefore, if A_{eff} is small compared to the EPR linewidth, then the maximum ENDOR response for transition $9\leftrightarrow10$ will be obtained for the magnetic-field value in the middle between the two EPR transitions, which coincides with the center of the overall EPR line ($g_{eff}\mu_B B$). In the experiment the field-stepped ENDOR technique was applied to determine the position of maximum ENDOR response of transition $9\leftrightarrow10$ for the most intense aluminum hyperfine-interaction shells. Figure 5 depicts the obtained results with the intensity expressed in arbitrary linear units. Also indicated, at the $B=0$ position, is the center of the overall EPR line as determined from the EPR experiment. As can be noted from the figure, the maxima determined for individual aluminum shells do not coincide. This effect has already been noted in the earlier ENDOR investigations and is responsible for line broadening due to the multispecies character of the Si-NL10 spectrum. The Si-NL10 spectrum is found to be a superposition of up to ten almost identical EPR components. In Fig. 5, also, the superposition of the EPR images generated by FSENDOR for all the aluminum shells as observed for this sample is depicted. The EPR images were simulated with Gaussian line shape and 0.1 mT width, as observed in the experiment. Following the remarks presented in Sec. I, one cannot expect that
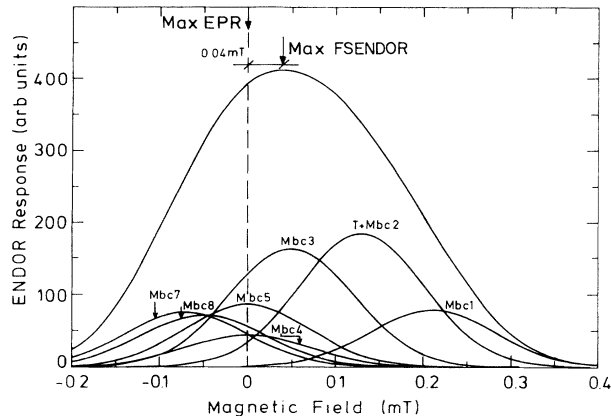
FIG. 5. Components of the EPR image as determined by the FSENDOR technique on the basis of the hyperfine interactions with the ^{27}Al nuclei following the 48-h 470 °C heat treatment. The difference between the field positions of the maximum of the original EPR line, at $B = 0$, and of the one obtained as the superposition of the FSENDOR determined components can be noted.

FIG. 6. Generation kinetics of the various Si-NL10-Al species as determined by the FSENDOR technique for the 470 °C heat-treatment temperature. For easy comparison the time dependence of the EPR line has also been depicted.

such a superimposed line would reproduce the intensity of the original EPR signal, since the information on the absolute intensity has been lost in the ENDOR experiment. Nevertheless, one can expect that the center of the FSENDOR reproduced superposition should coincide with that of the original EPR line at $B = 0$. As can be seen from Fig. 5, this is not the case, indicating therefore that not all the components of the total EPR line have been accounted for. The actual 0.04-mT difference between the two maxima as determined by Fig. 5 is comparable with the separations of individual species. Since the individual species could be resolved in the FSENDOR experiment, the field difference of this magnitude is considered to be meaningful.

In Fig. 6 the maximum ENDOR response as determined in the experiment for individual aluminum species, as well as the overall EPR intensity, is plotted as a function of the annealing time. The first data could be taken only after 17 h of heat-treatment time, since for shorter annealing the ENDOR signal-to-noise ratio was too low. As can be noted, all the aluminum shells exhibit kinetics identical to that of the overall EPR signal.

C. EPR of heavily aluminum-doped material

A somewhat different approach to the problem of aluminum involvement was exercised by following the generation kinetics of the Si-NL10 centers in Czochralski-grown silicon in which the aluminum doping was at the solubility-limit level. The results are presented in Fig. 7(a). For direct comparison Fig. 7(b) shows analogous data obtained in one of our earlier studies[4] for a silicon sample of similar oxygen contents and ≈ 20 times lower aluminum concentration. In the figures the generation kinetics of both TD-related EPR centers Si-NL8 and Si-NL10 is depicted; also the concentration of thermal donors as determined on the basis of room-temperature
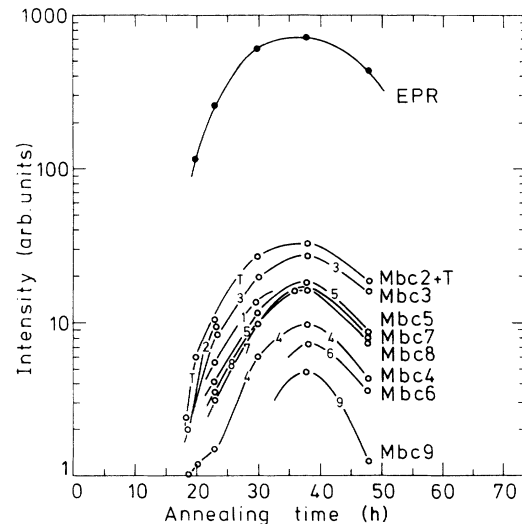
resistivity measurements is shown. Concentrations of the NL8 and NL10 centers were estimated using the calibrated reference sample.

IV. DISCUSSION

A. Si-NL10 and aluminum-oxygen complexes

As already stated in the Introduction, the question of aluminum incorporation in NL10 TD's is at the heart of the paper. ENDOR studies performed for the Si-NL10 center produced in boron- and phosphorus-doped silicon show, as expected, a total absence of any hyperfine interactions with aluminum.[16] The contradictory situation follows from the fact that the ENDOR study of that same spectrum, but produced in Al-doped samples, has actually revealed discrete hyperfine interactions with ^{27}Al nuclei. The present study addresses this problem.

We start with the notion that in aluminum-doped material thermal-donor generation is enhanced in comparison to silicon containing other p-type dopants, as first observed by Fuller, Doleiden, and Wolfstirn.[17] The enhancement was found to coincide with a similar increase of the production of Si-NL10 centers.[4] However, on the basis of a simple concentration argument, it appears impossible to admit the incorporation of aluminum atoms in the Si-NL10 centers in phosphorus- or boron-doped material; the contamination with aluminum in these materials was shown to be too low.[18] Nevertheless, the possibility of aluminum involvement could easily be investigated by drastically altering the aluminum concentration. This idea was followed by Claybourn and Newman,[13] who studied thermal-donor generation in heavily aluminum- and boron-doped silicon ([Al] $\approx 10^{17}$ cm^{-3}, [B] $\approx 7 \times 10^{16}$ cm^{-3}) with photoexcitation spectroscopy. They confirmed that substitutional acceptors are lost dur-

ing thermal-donor generation, the effect being far more pronounced for aluminum than for boron doping. Furthermore, in Al-doped material the photoionization spectra revealed the generation of additional donor centers. It was then tempting to identify these new donors as
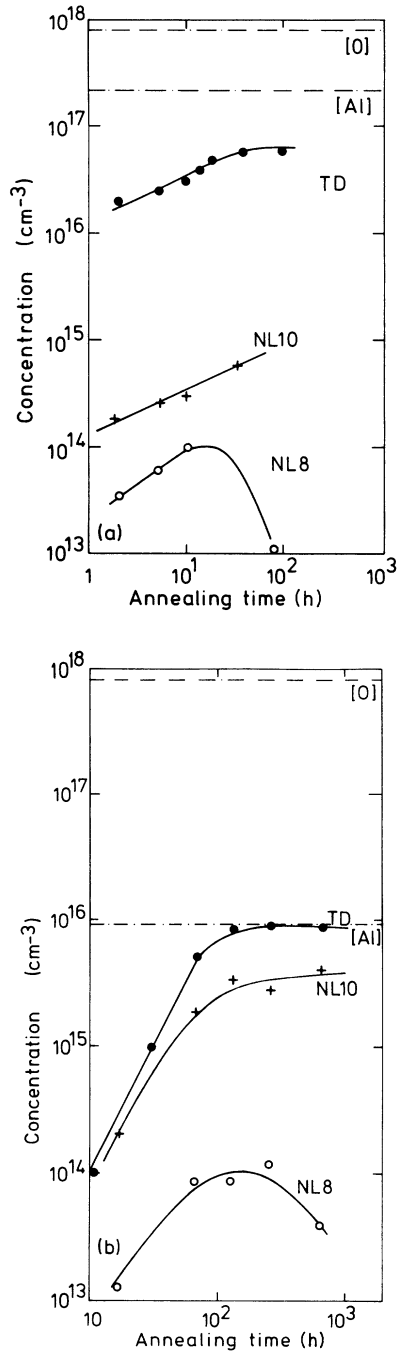
aluminum-oxygen complexes and correlate them with the Si-NL10 centers. The present study provides two independent arguments against such identification.

(1) EPR measurements on heavily aluminum-doped silicon ($[Al] \approx 2 \times 10^{17}$ cm^{-3}) as summarized in Sec. III C do not indicate a correlated enhancement of the production of Si-NL10 centers, when compared to the behavior of the material with a 20-times-lower aluminum content (see Fig. 7). The thermal-donor generation as depicted in these figures can be very well understood by a simultaneous occurrence of two processes: the removal of aluminum from the acceptor (substitutional) positions and generation of thermal-donor centers with the maximum concentration and generation kinetics dependent only on the available oxygen concentration.

(2) The field-stepped ENDOR results presented in Sec. III B show that the maximum of the total EPR image as determined by superimposing the FSENDOR results for *all* the aluminum shells observed in the experiment does not coincide with the maximum position of the real resonance line as found in a direct EPR measurement (see Fig. 5). This result shows that, in the aluminum ENDOR, not all the components of the total EPR line are represented. It indicates therefore the existence of more Si-NL10 species which contribute to the overall EPR signal but which do not possess an aluminum nucleus in their structure. Such result proves that a (partially) different variety of centers is taking part in both experiments. In this way there emerges indirect, but otherwise very convincing, evidence of the simultaneous existence of very similar Si-NL10 centers with and without aluminum participation.

What remains to be explained is why and how apparently some of the Si-NL10 species can contain aluminum in their structure and why this aluminum does not affect the measurable properties of the center. Alternatively, one may ask why the interactions with aluminum nuclei are observed only for the Si-NL10 centers generated in aluminum-doped material. Claybourn and Newman[13] showed that group III acceptors are lost from substitutional positions in the process of thermal-donor creation. Aluminum is known to be very vulnerable to the Watkins exchange mechanism[19] and is then by far the most easily removed shallow acceptor dopant. Further, the interstitial aluminum atoms can diffuse very rapidly through the silicon crystal.[20] It is possible that the interstitial aluminum atoms get trapped in the strain field produced by the oxygen clustering; some of these oxygen clusters will be eventually thermal donors, and will therefore have an aluminum atom trapped in the vicinity. Such a possibility seems especially probable in view of the reported ability of interstitial aluminum atoms to replace silicon atoms in the precipitates of silica during high-temperature heat treatment.[20] It may also be possible that the oxygen clustering starts favorably near substitutional aluminum atoms due to a locally higher oxygen concentration. The substitutional aluminum atom when closely surrounded by oxygen atoms would also no longer be visible in photoexcitation spectroscopy as a "normal" substitutional aluminum acceptor.

The shallow centers in silicon have delocalized charac-

FIG. 7. Generation kinetics of TD-related EPR centers in two different kinds of aluminum-doped, carbon-lean ($[C] \leq 5 \times 10^{15}$ cm^{-3}) silicon samples as used in the current study: (a) $[Al] \approx 2 \times 10^{17}$ cm^{-3} and $[O_i] \approx 8.5 \times 10^{17}$ cm^{-3}, (b) $[Al] \approx 9 \times 10^{15}$ cm^{-3} and $[O_i] \approx 7 \times 10^{17}$ cm^{-3}.

ter with the wave function spanning many shells of surrounding ligands. Deep centers are usually well localized within the nearest neighbors. However, for deep centers the wave function can also become considerably extended in particular directions, being then indicative of a strain field around the defect. This is the case of vacancy-based centers where the ENDOR investigation revealed the "chain character" of the wave function.[21] As a result of it, in the ENDOR study of a Si:V^- (Ref. 15), the hyperfine interactions with over 50 (silicon) ligand shells could be observed. The obviously delocalized character of the Si-NL10 center poses a question as to whether the experimentally observed hyperfine interactions with aluminum do not represent distant ligand ENDOR. In such a case the intensities could be considerably enhanced due to a higher ENDOR yield of the ^{27}Al nucleus compared to ^{29}Si. However, in this case one would expect to observe the signals from randomly distributed aluminum atoms. This is not the case, as the experiment reveals hyperfine interactions of well-defined magnitude with Al atoms located in one symmetry plane only. Therefore, the interpretation of the experimental data would require that either the electronic wave function is restricted to the single mirror plane or that the strain field formed around the Si-NL10 center traps the aluminum atoms on one site only in the single mirror plane. The existence of such a strain field and its effectiveness for trapping impurities are evidenced by the fact that oxygen atoms are only being positioned in the same plane.

B. Si-NL10 growth mechanism

The kinetics of the thermal-donor generation process is of crucial importance for the developing of the model of these centers. The most detailed results could be obtained here from the infrared studies,[2] since these were the only ones which could separate TD species and yield quantitative information on the concentration. From these studies it was concluded that thermal-donor centers had a form of gradually growing clusters. It was then naturally assumed that the thermal-donor growth occurred by addition of interstitial oxygen atoms.

In the ENDOR measurements of Michel et al.[22] an attempt was made to correlate Si-NL8 ENDOR-resolved species with the thermal-donor species as identified in the infrared. The authors could tentatively correlate their ENDOR species A as the infrared species (TD3)$^+$, while concluding that they failed to observe the first two species TD1 and TD2. A precise one-to-one correlation of TD species as revealed by ENDOR and infrared absorption was not possible. The ^{17}O ENDOR experiment on Si-NL8 showed that all the oxygen atoms participating in the structure of this center were contained within the symmetry planes of the center, but no oxygen atoms were identified on the twofold rotation axis. All of the five identified ENDOR species were shown to be of the orthorhombic symmetry. This particular finding has an important consequence for the thermal-donor growth mechanism. If the thermal-donor center would be growing by addition of a single oxygen atom, then, in order to maintain the orthorhombic symmetry, the additional ox-

ygen atoms could only be positioned along the twofold axis. Since no such oxygen interactions were observed, this could be only interpreted in that either the thermal-donor growth process did not take place or occurred by the simultaneous addition of two oxygen atoms (in the mirror plane). Such a growth mechanism appeared very improbable, especially in view of the extended size of the later thermal-donor species. On the other hand, in the case when the existence of the growth mechanism was questioned, some other process would have to be responsible for the multispecies character of TD's. Therefore, the Si-NL8 ENDOR study did not explain the thermal-donor growth mechanism.

In the Si-NL10 ENDOR experiment, generally a somewhat higher resolution could be obtained. In case of the ^{27}Al ENDOR study the quadrupole moment of the aluminum nucleus serves to magnify further the effect of the symmetry lowering. It is then possible to observe the experimental details which cannot be detected in the silicon and oxygen ENDOR. In the present ENDOR study a maximum of ten thermal-donor species was observed. It was surprising to note that all of them except one had monoclinic symmetry. It would have been more natural to observe an equal number of orthorhombic Si-NL10 species. Addition of the first oxygen atom lowers the symmetry, but addition of the second could restore the symmetry back to orthorhombic. One then has to conclude that either the thermal donor is not growing or the growth process, which can occur by subsequent addition of single oxygen atoms, is not symmetrical with respect to the aluminum atom.

The results of the current study as depicted in Fig. 6 also shed some light on the growth mechanism of the Si-NL10 center. These results should be compared with the kinetics of individual TD species as determined from the infrared studies,[2] on the basis of which the most prominent TD models have been developed.[23] The results of Fig. 6 contradict the idea of a subsequent growth of thermal-donor centers. The measured kinetics show that all the species grow parallel in time and all attain their (different) maximal concentrations for the same heat-treatment time. The results would then practically exclude any growth mechanism, in the sense that the "later" species is created from the "earlier" one. Therefore, a different explanation of the multispecies character of the Si-NL10 thermal-donor center is required, posing again the basic question of the distinction between the many experimentally identified species. The fact that not all the species are observed for every heat-treatment time value (and especially in the beginning, when the different species seem to appear subsequently) would then be due entirely to the limited sensitivity of the EPR (and, consequently, ENDOR) experiment, where the center has to pass a certain concentration threshold value in order to be observable.

The results presented in Fig. 6 are difficult to reconcile with the interpretation of the g shifting effect, as observed for both TD-related spectra.[4] According to this interpretation, g shifting is caused by the different ratios of concentration of various TD species in different phases of the heat treatment. As can be concluded from Fig. 6, the

concentration ratio between the "early" and the "late" TD species changes only very slightly during the heat treatment and consequently can give rise only to a limited transformation of the observed averaged g parameter.

It should nevertheless be realized that the g-shifting mechanism may indeed be more complex and generated by a simultaneous action of several different and mutually independent mechanisms. During the heat treatment of p-type Czochralski silicon, not only are thermal-donor centers generated but also the acceptors initially present in the material are being removed. Such a process leads to continuous change of the Fermi-level position in the sample and therefore will also affect the paramagnetism of the Si-NL10 and Si-NL8 centers, giving rise to an effect indistinguishable from subsequent generation of the more shallow species. Yet another possible mechanism giving rise to the semicontinuous change of the g value of the superimposed EPR spectrum in the aluminum-doped material would be the time-varied ratio of the Si-NL10 species which do and which do not contain aluminum. In this case the g shifting would be related to aluminum doping; the fact that the phenomenon can be observed for other dopants as well poses a question as to whether or not other impurities could also participate in the structure of (Si-NL10) thermal donors.

V. CONCLUSIONS

In this study the problem of aluminum incorporation in the Si-NL10 thermal-donor center has been addressed.

The investigations performed on heavily aluminum-doped silicon showed that the Si-NL10 centers cannot be uniquely identified as oxygen-aluminum complexes as observed by Claybourn and Newman.[13] The ENDOR study unraveled the existence of ten different Si-NL10 species; out of these, only one has orthorhombic symmetry and the other ones are monoclinic. The FSENDOR study provided evidence that in aluminum-doped Czochralski silicon also Si-NL10 centers which do not exhibit hyperfine interaction with ^{27}Al nuclei created. The generation kinetics of the Si-NL10 centers as determined on the basis of this study appears to be in contradiction with current knowledge about the thermal-donor centers and questions the idea that subsequent growth of Si-NL10 occurs by diffusion-governed addition of oxygen or any other component.

Although the exact role of the aluminum atoms in the formation of the Si-NL10 centers is not fully clarified, it appears that even in the case when ^{27}Al ENDOR can be experimentally observed, the aluminum atoms do not form the core of the Si-NL10 center and do not have any significant influence on the electronic structure of the core.

ACKNOWLEDGMENT

[1] A. Bourret, in *Proceedings of the Thirteenth International Conference on Defects in Semiconductors,* edited by L. C. Kimerling and J. M. Parsey, Jr. (TMS-AIME, New York, 1985), p. 129.

[2] P. Wagner and J. Hage, Appl. Phys. A **49**, 123 (1989).

[3] S. H. Muller, M. Sprenger, E. G. Sieverts, and C. A. J. Ammerlaan, Solid State Commun. **25**, 987 (1978).

[4] T. Gregorkiewicz, D. A. van Wezep, H. H. P. Th. Bekman, and C. A. J. Ammerlaan, Phys. Rev. B **35**, 3810 (1987).

[5] T. Gregorkiewicz, D. A. van Wezep, H. H. P. Th. Bekman, and C. A. J. Ammerlaan, Phys. Rev. Lett. **59**, 1702 (1987).

[6] J. Michel, J. R. Niklas, and J.-M. Spaeth, in *Defects in Electronic Materials,* edited by M. Stavola, S. J. Pearton, and G. Davies (Materials Research Society, Pittsburgh, 1988), p. 185.

[7] K. M. Lee, J. M. Trombetta, and G. D. Watkins, in *Microscopic Identification of Electronic Defects in Semiconductors,* edited by N. M. Johnson, S. G. Bishop, and G. D. Watkins (Materials Research Society, Pittsburgh, 1985), p. 263.

[8] T. Gregorkiewicz, H. H. P. Th. Bekman, and C. A. J. Ammerlaan, Phys. Rev. B **38**, 3998 (1988).

[9] J. Michel, J. R. Niklas, and J.-M. Spaeth, Phys. Rev. B **40**, 1732 (1989).

[10] T. Gregorkiewicz, H. H. P. Th. Bekman, and C. A. J. Ammerlaan, Phys. Rev. B **41**, 12 628 (1990).

[11] H. H. P. Th. Bekman, T. Gregorkiewicz, and C. A. J. Ammerlaan, Phys. Rev. Lett. **61**, 227 (1988).

[12] W. Burger, K. Lassman, C. Holm, and P. Wagner, in *Proceedings of the Eighteenth International Conference on the Physics of Semiconductors, Stockholm, Sweden, 1986,* edited by O. Engström (World Scientific, Singapore, 1986), Vol. 2, p. 851.

[13] M. Claybourn and R. C. Newman, Mater. Sci. Forum **38-41**, 613 (1989).

[14] T. Gregorkiewicz, H. E. Altink, and C. A. J. Ammerlaan, Acta Phys. Pol. A **80**, 161 (1991).

[15] M. Sprenger, S. H. Muller, E. G. Sieverts, and C. A. J. Ammerlaan, Phys. Rev. B **35**, 1566 (1987).

[16] J. Michel, N. Meilwes, J. R. Niklas, and J.-M. Spaeth, in *Shallow Impurities in Semiconductors, 1988,* edited by B. Monemar, IOP Conf. Proc. No. 95 (Institute of Physics, Bristol, England, 1989), p. 201.

[17] C. S. Fuller, F. H. Doleiden, and K. Wolfstirn, J. Phys. Chem. Solids **13**, 187 (1960).

[18] E. C. Lightowlers and R. C. Newman (private communication).

[19] G. D. Watkins, *Radiation Damage in Semiconductors* (Dunod, Paris, 1965), p. 97.

[20] R. Baron, G. A. Shifrin, O. J. Marsh, and J. W. Mayer, J. Appl. Phys. **40**, 3702 (1969).

[21] E. G. Sieverts, M. Sprenger, and C. A. J. Ammerlaan, Phys. Rev. B **41**, 8630 (1990).

[22] J. Michel, J. R. Niklas, J.-M. Spaeth, and C. Weinert, Phys. Rev. Lett. **57**, 611 (1986).

[23] A. Ourmazd, W. Schröter, and A. Bourret, J. Appl. Phys. **56**, 1670 (1984).